DNS of Active Control of Disturbances in a Blasius Boundary Layer

C. Gmelin, U. Rist and S. Wagner

Institut für Aerodynamik und Gasdynamik,
Universität Stuttgart, Pfaffenwaldring 21, D-70550 Stuttgart, Germany

Abstract. Many approaches with the objective to actively delay the laminar-turbulent transition in boundary layers are currently under investigation. These approaches, which are mostly based on the superposition of anti-phase disturbances fail in cases where high (nonlinear) disturbance amplitudes occur. One possible solution to overcome this problem is the direct feedback of instantaneous flow signals from the wall. In our case the spanwise vorticity (ω_z) on the wall is sensed, multiplied by a certain factor A and prescribed as a new boundary condition at the wall with some time delay Δt. This procedure (called $\boldsymbol{\omega_z}$**-control**) yields a robust algorithm which is less influenced by nonlinearities than other processes based on the linear superposition of disturbances (waves). The method was developed and evaluated using both linear stability theory and a three-dimensional spatial DNS code solving the complete Navier-Stokes equations.

1 Introduction

The most popular approach controlling transition is the superposition of disturbances with opposite phase to the existing waves. First attempts have been published by Milling [1], Liepmann et al. [2][3] and Kozlov et al. [4]. Until now this strategy has been realized many more times both experimentally [5] and numerically [6]. For disturbances with small (linear) amplitude a reduction in amplitude of up to 90% even in experiments is achievable. In contrast to their excellent performance in early transition stages these approaches don't work in a satisfactory manner in cases where high amplitudes occur due to nonlinear effects superposing disturbance and control wave. Moreover, the generation of large control waves which are necessary to cancel the initial wave with the aid of a suction/blowing slot sometimes causes very high velocities in the vicinity of these actuators, an effect which favors nonlinearities furthermore. These arguments make clear that there is a need for a smooth, robust control algorithm which is almost independent of the amplitude of the initial disturbance.

Several attempts have been made to control turbulent flows. Control via affection of the vorticity flux at the wall has been proposed by Koumoutsakos [7][8] whereas Choi, Moin & Kim [9] observed a damping effect on turbulent flows feeding back the instantaneous wall-normal velocity at a certain distance from the wall to the boundary. They report the establishing of a "virtual wall", i.e. a plane that has approximately no through-flow halfway between

the detection plane and the wall and therefore a drag reduction of 25% and a strong reduction of turbulent flow structures. In some aspects our approach is very similar to their idea of feedback of instantaneous signals but in most cases flow data of the whole flow field is not available. In our case this problem is handled by sensing the spanwise vorticity at the wall, present as wall shear stress and easily measurable by hot film sensors or cavity hot wires [10], for example. These signals are multiplied with a certain factor and prescribed as wall-normal velocity v at the wall (for a detailed description see below in section 4).

An approach complementary to our LST investigations (section 5) has been applied by Joshi et al. [11] for plane Poiseulle flow using the spanwise shear at the wall as sensor variable and blowing/suction for actuation, as well. However, they converted the problem into a control theoretical one and determined the effect of the feedback control by the position of the zeros and poles of the system. Furthermore, they obtained an optimal sensor location relative to the actuator similar to our most effective phase shift between sensing and actuation. Another contribution concerning feedback control, again in planar Poiseulle flow was published by Hu et al. [12]. Analogical to our approach they modified the Orr-Sommerfeld equation to get some information about the stability of the controlled flow system. In contrast to the actuation via blowing/suction at the wall used in our investigations they modulated the wall temperature periodically to alter the viscosity of the fluid and therefore to stabilize the flow.

In our paper we use Direct Numerical Simulations (DNS) and Linear Stability Theory (LST) to explore the concept of ω_z-control and to evaluate its effects on the disturbances involved in the laminar-turbulent transition in a Blasius boundary layer. The DNS method and a discussion of results in the linear regime are presented in section 2 and 4, investigations using LST in section 5, active control of nonlinear disturbances in section 6 and a summary is given in section 7.

2 Numerical Method

All simulations were performed in a rectangular integration domain with the spatial DNS-code developed by Konzelmann, Rist and Kloker [13][14][15].

The flow is split into a steady 2D-part (Blasius base flow) and an unsteady 3D-part. The x-(streamwise) and y-(wall-normal) directions are discretized with finite differences of fourth-order accuracy and in the spanwise direction z a spectral Fourier representation is applied. Time integration is performed by the classical fourth-order Runge-Kutta scheme. The utilized variables are normalized with $\tilde{U}_\infty = 30\frac{m}{s}$, $\tilde{\nu} = 1.5 \cdot 10^{-5}\frac{m}{s^2}$ and $\tilde{L} = 0.05m$ ($\tilde{}$ denotes

dimensional variables):

$$x = \frac{\tilde{x}}{\tilde{L}} \quad y = \frac{\tilde{y}}{\tilde{L}} \quad z = \frac{\tilde{z}}{\tilde{L}} \quad t = \tilde{t} \cdot \frac{\tilde{U}_\infty}{\tilde{L}}$$
$$u = \frac{\tilde{u}}{\tilde{U}_\infty} \quad v = \frac{\tilde{v}}{\tilde{U}_\infty} \quad w = \frac{\tilde{w}}{\tilde{U}_\infty} \quad Re = \frac{\tilde{U}_\infty \tilde{L}}{\tilde{\nu}} = 10^5 \quad ,$$

where u, v and w are the components of the unsteady velocity disturbances. This leads to the dimensionless frequency $\beta = 2\pi\tilde{f}\tilde{L}/\tilde{U}_\infty$, where $\tilde{f}$ is the frequency in $[Hz]$ and the dimensionless spanwise vorticity $\omega_z = \partial u/\partial y - \partial v/\partial x$. The Reynolds numbers formed with the displacement thickness are $Re_{\delta_1} \approx 500$ at the inflow boundary and $Re_{\delta_1} \approx 1300$ at the outflow boundary.

3 Computational aspects

Clearly the present work aims at gaining insight into new laminar-flow control strategies through numerical simulation. The necessary numerical tools have been developed and optimised for efficient use of the available resources earlier [16]. Due to their speed and the available large memory of the supercomputers of the HLRS either more computations were possible within a given time frame or specific cases could be analysed more thoroughly. Even our computations of eigenvalues in the framework of linear stability analysis profited from the computational advantages of the supercomputers compared to workstations. The spanwise Fourier ansatz principally reduces the 3-D problem in physical space to a set of $(K+1)$ complex 2-D problems in Fourier space thus enabling a largely parallel computation in Fourier space. However, the modes are coupled by the nonlinear convective terms of the vorticity transport equations and are transformed to physical space ("pseudospectral method" with de-aliasing procedure) for the calculation of the nonlinear vorticity terms, which in turn are parallelized in streamwise direction.

The uniform equidistant grid in $x-$ and $y-$ direction contains maximal 2882×241 points using up to 25 Fourier modes in spanwise direction. The problem has been computed on the hww-supercomputer, the NEC SX-5 (16 processors, 32 GB RAM) using approximately 5 GB RAM. The code reaches a performance of up to 1.6 GFLOPS at a vector operation ratio of 99.4% resulting in a computation time of $\approx$2.0 μs per gridpoint, time step and spanwise harmonic mode and a memory requirement of about 350 Byte per point and spanwise mode. About 88% of the overall time was spent in parallel execution and only 12% of the total computation time for I/O, system-calls and serial program parts. On the other hand, the investigations concerning linear stability theory (chapter 5) were conducted on another hww supercomputer, the NEC-SX-4 running serial using approximately 20MB RAM. Single eigenvalues have been calculated interactively.

The amount of accumulated data is approximately 2 GB per run but this value strongly depends on the case, the number of stored timesteps, and the

resolution. Therefore it is very important to have the opportunity to store and to access the data rapidely. A very significant point in this context is the direct connection between the hww-supercomputers and the hww-fileserver, the hwwfs1 enabling a very fast exchange of data.

4 Control Mechanism

To actively damp disturbances in boundary layers we use the feedback of instantaneous signals of the spanwise vorticity fluctuations measured at the wall. These signals are multiplied by an amplitude factor $|A|$ and are prescribed as a v-boundary condition after a time delay Δt at the wall which is necessary to produce the phase shift Φ shown in Fig.1.

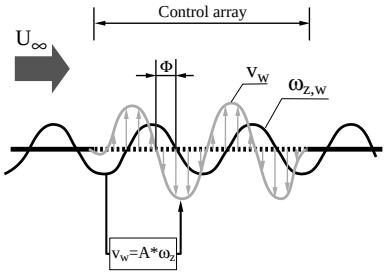

Fig. 1. Ilustration of the ω_z-control principle

The effects of changing $|A|$ and Δt resp. Φ will be studied in section 5 using linear stability theory. Here, results of DNS are analyzed in order to show how the method works in the linear case. For a small-amplitude 2D Tollmien-Schlichting (TS-) wave results of three simulations are compared with each other in Fig.2. Compared to the uncontrolled case there is a strong damping effect of the ω_z-control on the disturbance amplitude in Fig.2 (a). Because of the small amplitudes a linear superposition of waves is valid here, i.e. the controlled wave (——) in Fig.2 (a) can also be viewed as the addition of the uncontrolled wave (-·-·-·-) with a control wave which arises when previously extracted v_w (index w denotes wall quantities) signals are prescribed in an otherwise undisturbed flow (- - - -).

However, this approach has to be clearly distinguished from the "classical" wave superposition principle [5], where an anti-phase disturbance of the same frequency and wave number is superposed to the initial perturbation. In the "classical" case, frequency and wave number of both disturbances are the same. Looking at the wave numbers of the present example in Fig.2 (b) one can clearly see, that this is not the case here using the ω_z-control, because the wave number α_R and therefore the phase velocity c_{ph} of the controlled wave is strongly different from the uncontrolled case.

A deeper insight into the acting mechanisms can be obtained by looking at the spatial linear 2D energy balance equation. This equation is derived from the 2D Navier-Stokes equations with the aid of a parallel flow assumption and a wave approach for the disturbances [17] [18]. Flow properties are split into steady mean and fluctuating quantities. Velocities in streamwise (x), wall normal (y) and spanwise (z) direction are $u = U + u'$, $v = V + v'$, $w = w'$, $\omega_Z = \Omega_z + \omega_z'$, respectively. Overlines denote the average over one period of

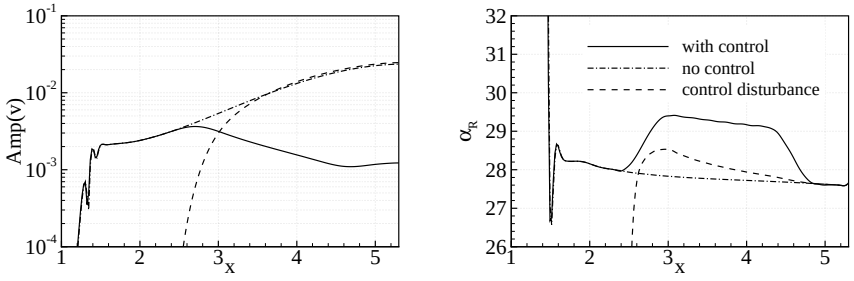

Fig. 2. v-Amplitude (a) and wave number (b) of undisturbed linear wave, controlled wave and control disturbance. Control parameters: $|A| = 7.5 \cdot 10^{-5}$, $\Delta t = 0 \Rightarrow \Phi = 0$, control array from $x = 2.4 \ldots 4.8$. Control disturbance is obtained by an extra simulation prescribing the wall signal of the run with control at the wall without initial disturbance. Due to the presence of linear waves addition of modes is valid.

time.

$$E = \frac{d}{dx}\int_0^\infty \frac{1}{2}U(\overline{u'^2} + \overline{v'^2})dy = R + D + P + \underbrace{-\nu\frac{d}{dx}\int_0^\infty \overline{v'\omega_z'}\,dy - \int_0^\infty (\overline{u'^2} - \overline{v'^2})\frac{\partial U}{\partial x}\,dy + \overline{v_w' p_w'}}_{\text{small}} \tag{1}$$

E is the spatial rate of increase of the fluctuation energy flux. $E > 0$ indicates a growth of disturbances whereas $E < 0$ means a weakening of disturbances. The terms which form the major part of the right hand side of equation (1) are

- the energy production term, where $\overline{u'v'}$ is the averaged Reynolds stress

$$R = \int_0^\infty -\overline{u'v'}\Big(\underbrace{\frac{\partial U}{\partial y}}_{>0} + \underbrace{\frac{\partial V}{\partial x}}_{\to 0}\Big)dy \quad , \tag{2}$$

- the dissipation

$$D = -\nu\int_0^\infty \overline{\omega_z'^2}\,dy \quad , \tag{3}$$

- and the pressure term

$$P = -\frac{1}{\rho}\frac{d}{dx}\int_0^\infty \overline{p'u'}\,dy \quad . \tag{4}$$

All integrals are solved by integrating the flow quantities from the wall to the upper edge of the integration domain using finite differences of fifth order accuracy. The error obtained by solving the integrals not to infinity is negligible because the integrands are already very close to zero at the upper boundary.

The application of ω_z-control at $x > 2.5$ changes the sign of E together with the curves for R and P (Fig.3). Clearly, the energy production term R dominates the complete energy balance. Its sign, respectively the sign of the Reynolds stress $\overline{u'v'}$ (see eqn.2), determines the sign of the whole right-hand side of equation (1) and therefore the attenuation or growth of the regarded disturbance ($\overline{u'v'} > 0 \Rightarrow R < 0 \Rightarrow E < 0 \Rightarrow$ reduction of amplitude and vice versa). The first of the two remaining terms, the dissipation term D has always a damping effect whereas the pressure term P always tends to counteract the production term R.

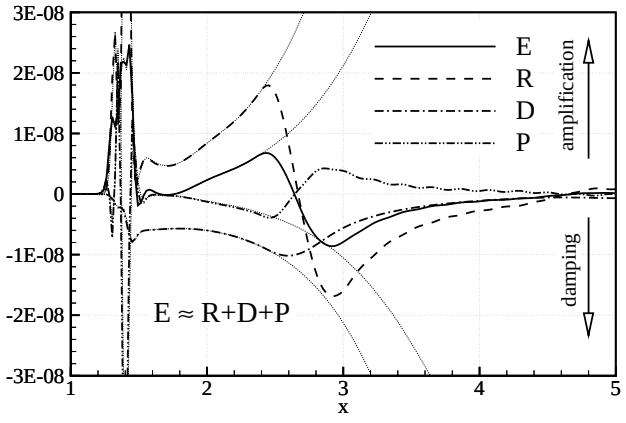

Fig. 3. Streamwise distribution of the main energy-balance terms based on eqn.(1), dotted lines: uncontrolled case for reference.

The change of sign of the Reynolds stress $\overline{u'v'}$ when control is applied is not caused by different u' or v' amplitudes but by its strong sensitivity to the phase difference $\Delta\Theta = |\Theta(u') - \Theta(v')|$ around $\Delta\Theta(y) = \frac{\pi}{2}$ [19] which is altered by the non-zero v_w.

5 Linear Stability Theory

To get an overview of the damping capabilities of the present concept and to optimize the parameters for further simulations, investigations using linear

stability theory (LST) were performed. Therefore, the boundary conditions at the wall for the Orr-Sommerfeld (and Squire equation) had to be changed (index w denotes wall properties) to

$$v'_w = A \cdot \omega'_{z,w} \tag{5}$$

$$v'_w = A \cdot \left(\frac{\partial u'}{\partial y} - \frac{\partial v'}{\partial x} \right)$$

$$(1 + iA\alpha) \cdot v'_w - A \cdot \left(\frac{\partial}{\partial y} \right)_w u' = 0 \tag{6}$$

$$\text{with} \quad A = |A| \cdot e^{i\Phi}$$

where $|A|$ is the amplitude factor and Φ is the phase difference between v_w and $\omega_{z,w}$ similar to the time delay used in the simulations. Due to the ability to express ω_z in terms of u and v (eqn. 6) the discretized system remains a homogeneous eigenvalue problem which can be solved in the same way as the original Orr-Sommerfeld equation.

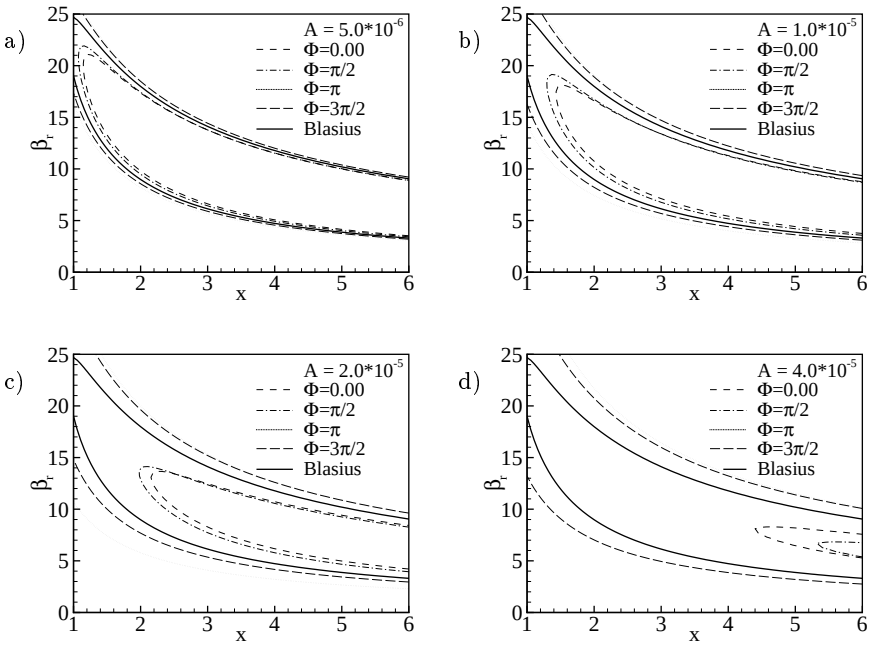

Fig. 4. Curves of zero amplification ($\alpha_i = 0$) for 2D-TS-modes with different control parameters. (a): $|A| = 5 \cdot 10^{-6}$, (b): $|A| = 1 \cdot 10^{-5}$, (c): $|A| = 2 \cdot 10^{-5}$, (d): $|A| = 4 \cdot 10^{-5}$.

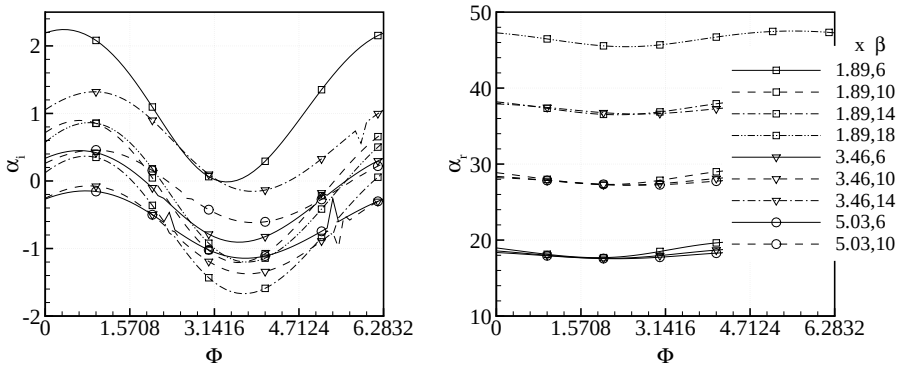

Fig. 5. Wave number α_R and amplification rate α_I from LST with ω_z-control ($v_w = |A| \cdot e^{i\Phi} \cdot \omega_{z,w}$) applied. $|A| = 2 \cdot 10^{-5}$ (Note that for the spatial approach $\alpha_i < 0$ means amplification.)

A strong damping effect and a significant reduction of the unstable area in the stability diagram (Fig.4) is already caused by very small amplitudes $|A|$.

Results of a detailed investigation of the influence on the most unstable eigenvalues are presented in Fig.5 for an amplitude of $2 \cdot 10^{-5}$ and all possible phase angles Φ between v_w and $\omega_{z,w}$. One can see that the largest possible damping for all modes appears in the region of $\Phi \approx \frac{\pi}{4} ... \frac{\pi}{2}$.

6 Active Control of Nonlinear Disturbances

As a test case for the effect of the ω_z-approach on disturbances with large amplitude a typical K-breakdown scenario (dotted lines in Fig.6 a)) is used where a fundamental mode (1,0) with large amplitude and a stationary disturbance (0,1) (the first index denotes multiples of the frequency β, the second multiples of the basic spanwise wave number $\gamma = 20$) are excited initially. Because of nonlinear interactions the 3D-mode (1,1) arises and falls in resonance with the fundamental 2D-mode (modes (1,0) and (1,1) share the same wave number from $x \approx 3.4 \ldots 4.0$ cf. Fig.6 b), dashed lines). The other modes shown are due to nonlinear combinations. They demonstrate transition to turbulence by generation of higher harmonics and the mean flow distortion (0,0). When the strongly amplified 3D-waves have reached the amplitude level of the fundamental mode, saturation sets in and transition to turbulence takes place (dashed lines). Applying ω_z-control to this scenario two main control effects can be distinguished: direct damping of nonlinear disturbances and the affection of the resonant behaviour. The first is comparable to the linear case where ω_z-control was shown to be able to directly damp TS-disturbances.

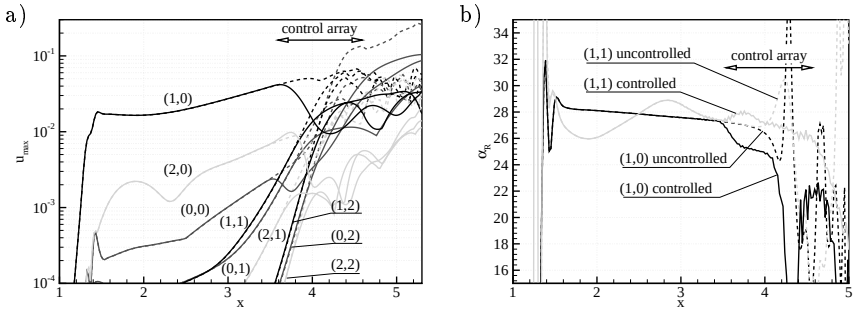

Fig. 6. K-breakdown, u_{max}-amplitudes vs. x. Only 2D-modes controlled ($|A| = 2 \cdot 10^{-4}$, $\Phi \approx \frac{\pi}{2}$). a) u_{max}-amplitudes, dashed lines: uncontrolled case, grey lines: higher harmonics. b) wavenumbers

In Fig.6 only 2D modes, i.e. (1,0) and its higher harmonics were actively controlled with a phase Φ of approximately $\frac{\pi}{2}$ applied by a fixed time delay between $\omega_{z,w}$ and v_w (control array from $x = 3.5$ to $x = 4.6$). Despite the strongly nonlinear regime in this case the amplitudes of the 2D modes (1,0) and (2,0) are strongly decreased.

The damping of the 3D-modes is now due to the second effect mentioned above: resonance in 2D boundary layers is accompanied by phase synchronization of the resonant (1,1) to the fundamental (1,0) mode (i.e. both waves have the same phase speed $c = \frac{\beta}{\alpha_{\text{fundamental}}}$). Investigations using LST predict apart from changed amplification rates strongly altered wave numbers of the controlled mode (Fig.5). This effect leads to a decoupling of the resonant modes and can therefore suppress resonance. Fig.6 b) shows the wave numbers of the most important modes of the simulation mentioned above. Before the direct attenuation via ω_z-control can take effect the wave number of mode (1,0) is shifted to lower values (i.e. the wave is accelerated), the resonant mode (1,1) is not synchronized any more and resonance between (1,0) and (1,1) is prevented.

Looking at Fig. 5 one can observe that the optimal phase shift between ω_z and v is more or less independant of the frequency. Thus controlling with a fixed time delay between sensor and actuator signal yields to a different, non optimal control phase for every frequency. To obtain the desired Phase for every occuring frequency resp. wave number, we applied a spatial *FIR-Filter* of length l to the input data to treat every wavenumber in the proper way:

$$v_w(x,t) = |A| \sum_{x'=x-l/2}^{x+l/2+1} \underbrace{h(x'-x+\frac{l}{2}+1)}_{i(\text{Fig. 7})} \cdot \omega_{z,w}(x',t) \tag{7}$$

Transformed in Fourier space we obtain:

$$V_w(x,\alpha) = A \cdot H(\alpha) \cdot \Omega_{z,w}(x,\alpha) \tag{8}$$

where V_w, H and $\Omega_{z,w}$ are the transformed v_w, h and $\omega_{z,w}$. The input data vector consisting of data from $x - l/2$ to $x + l/2$ is multiplied with the filter vector h. In Fourier space the input signal is multiplied by a complex transfer function to obtain the output v_w-signal. Thus, it is possible to filter the input data dependent of its spatial wavenumber and to choose the optimal phase relation for every mode. An additional, desired effect is the prevention of instabilities, which might be introduced unintentionally by the actuator response to the flow field. Without the use of the present filter, above a certain amplitude level $|A|$ of approximately $2.5 \cdot 10^{-4}$ the occurence of high-frequency instabilities can superseed the active attenuation of instabilities and produce large amplification of all modes by nonlinear interaction.

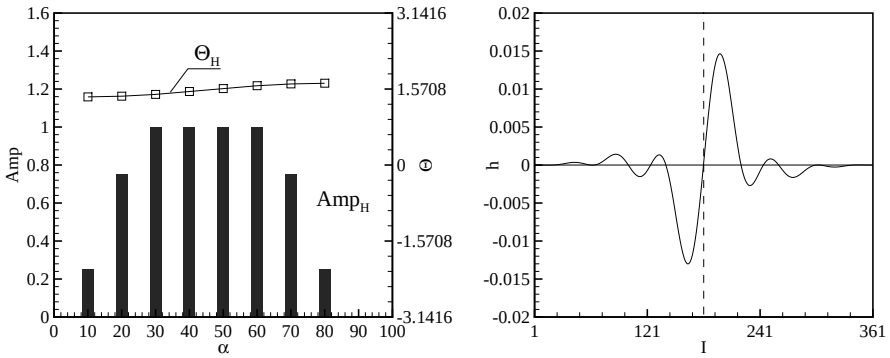

Fig. 7. Transfer function and filter coefficients of the spatial FIR-filter used to stabilize the ω_z-control.

Looking at further investigations applying ω_z-control in combination with a spatial filter in late nonlinear stages to both 2D and 3D modes shows that an amplitude reduction of more than one order of magnitude is possible. Fig.8 shows a simulation with control of the 2D (..,0) *and* 3D (..,1) modes where the control array extends from $x = 3.5$ to $x = 5.0$. Compared to previous simulations a further reduction of the disturbances is observed and larger control amplitudes are possible without the danger of undesirable high-frequency instabilities. The control amplitude is turned on via a spatial ramp function shown in Fig.8. With such an arrangement it is possible to prevent the occurence of transitional structures such as Λ-vortices or high shear layers when active control is applied only two wavelengths prior to their first appearence in the uncontrolled case (Fig. 9). As with other unsteady control

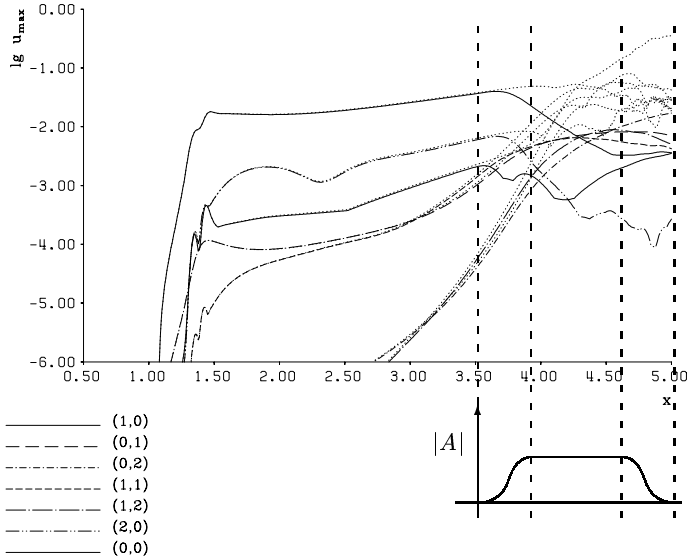

Fig. 8. K-breakdown, u_{max}-amplitudes vs. x. 2D- and 3D- modes controlled, application of a spatial FIR-filter ($|A| = 3 \cdot 10^{-4}$). Dotted lines: uncontrolled case. Small picture: Amplification factor $|A|$ vs. x.

strategies ω_z-control exhibits one shortcoming: stationary modes are not affected directly. Only by damping the fluctuating parts of the disturbance the nonlinear generation of these modes can be inhibited.

7 Summary

With the aid of Direct Numerical Simulations (DNS) it was possible to develop a simple, yet effective control algorithm to actively control the laminar-turbulent transition occurring in a 2D boundary layer. It combines two main effects: the direct attenuation caused by a change of the energy properties and a reduced resonance according to an altered phase velocity of the involved modes. Calculations using Linear Stability Theory (LST) show a strong dependence of the resulting wave number and amplification rate on the chosen amplitude and phase difference between ω_z' (sensed) and v_{wall}' (stimulated).

It is shown that this approach works very well even close to transition where the boundary layer instabilities have reached a highly nonlinear stage. Further investigations have to show how far transition can be shifted downstream and whether a complete relaminarisation of the flow is possible using this approach.

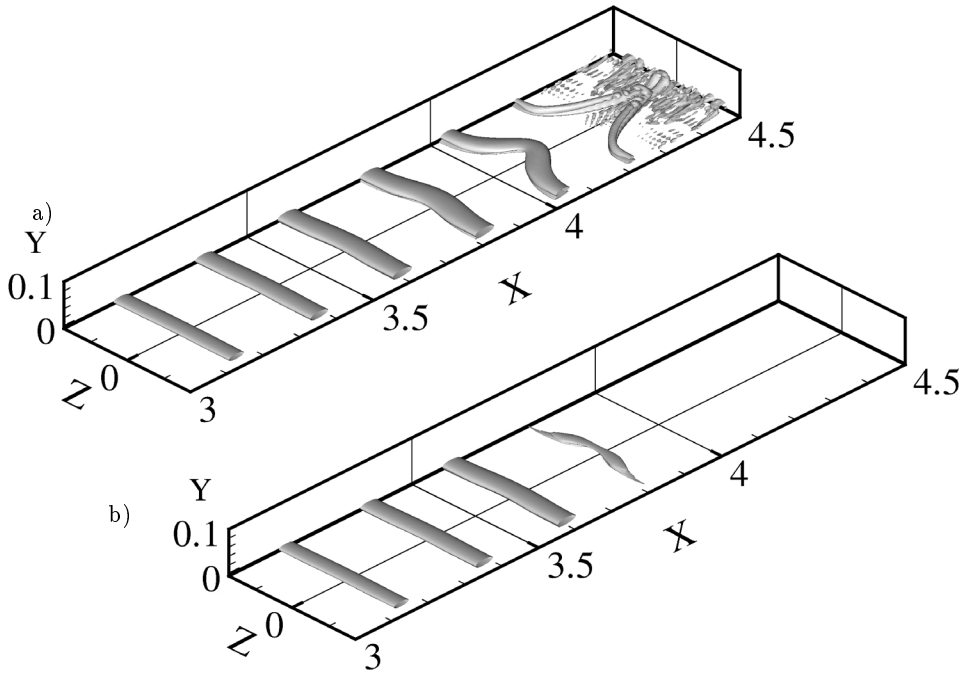

Fig. 9. Instantaneous vortex structures made visible by the λ_2-Criterium [20] for the uncontrolled case (a) and the controlled case (b), same case as Fig.8

8 Acknowldgements

The support of this research work by the Deutsche Forschungsgemeinschaft DFG is gratefully acknowledged.

References

1. R. W. Milling. Tollmien-Schlichting wave cancelation. *Phys. Fluids*, 24:979–981, 1981.
2. H. W. Liepmann, G. L. Brown, and D. M. Nosenchuck. Control of laminar-instability waves using a new technique. *J. Fluid Mech.*, 118:187–200, 1982.
3. H. W. Liepmann and D. M. Nosenchuck. Active control of laminar-turbulent transition. *J. Fluid Mech.*, 118:201–204, 1982.
4. V. V. Kozlov and V. Y. Levchenko. Laminar-turbulent transition control by localized disturbances. In H. W. Liepmann and R. Narasimha, editors, *Turbulence Managment and Relaminarisation*. Springer Verlag, Berlin, Heidelberg, 1987. IUTAM-Symposium, Bangalore, India, 1987.
5. M. Baumann and W. Nitsche. Investigations of active control of Tollmien-Schlichting waves on a wing. In R.A.W.M. Henkes and J.L. van Ingen, editors, *Transitional Boundary Layers in Aeronautics*, volume 46, pages 89–98. KNAW, Amsterdam, North Holland, 1996.

6. E. Laurien and L. Kleiser. Numerical simulation of boundary-layer transition and transition control. *J. Fluid Mech.*, 199:403–440, 1989.
7. P. Koumoutsakos. Active control of vortex - wall interactions. *Phys. Fluids*, 9, 1997.
8. P. Koumoutsakos, T. R. Bewley, E. P. Hammond, and P. Moin. Feedback algorithms for turbulence control - some recent developments. AIAA 97-2008, 1997.
9. H. Choi, P. Moin, and J. Kim. Active turbulence control for drag reduction in wall-bounded flows. *J. Fluid Mech.*, 262:75–110, 1994.
10. M. Baumann, D. Sturzebecher, and W. Nitsche. On active control of boundary layer instabilities on a wing. In H.J. Heinemann W. Nitsche and R.Hilbig, editors, *Notes on Numerical Fluid Mechanics II*, volume 72, pages 22–29. Vieweg-Verlag, Braunschweig, 1998.
11. S. S.Joshi, J. L. Speyer, and J. Kim. A system theory approach to the feedback stabilization of infinitesimal and finite-amplitude disturbances in plane poiseulle flow. *J. Fluid Mech.*, 332:157–184, 1997.
12. H. H. Hu and H. H. Bau. Feedback control to delay or advance linear loss of stability in planar Poiseulle flow. In *Proc. R. Soc. London*, volume 447, pages 299–312, 1994.
13. M. Kloker. *Direkte Numerische Simulation des laminar-turbulenten Strömungsumschlages in einer stark verzögerten Grenzschicht.* Dissertation, Universität Stuttgart, 1993.
14. U. Konzelmann. *Numerische Untersuchungen zur räumlichen Entwicklung dreidimensionaler Wellenpakete in einer Plattengrenzschicht.* Dissertation, Universität Stuttgart, 1990.
15. U. Rist and H. Fasel. Direct numerical simulation of controlled transition in a flat-plate boundary layer. *J. Fluid Mech.*, 298:211–248, 1995.
16. P. Wassermann, M. Kloker, and S. Wagner. DNS of laminar-turbulent transition in a 3-D aerodynamics boundary-layer flow. In E. Krause and W. Jäger, editors, *High performance Computing in Science and Engineering.* Springer, 2000.
17. F. R. Hama, D. R. Williams, and H. Fasel. Flow field and energy balance according to the spatial linear stability theory of the Blasius boundary layer. In *Laminar-Turbulent Transition.* Springer-Verlag, 1980. IUTAM Symposium Stuttgart/Germany, 1979.
18. F. R. Hama and S. de la Veaux. Energy balance equations in the spatial stability analysis of boundary layers with and without parallel-flow approximation. Princeton University, Princeton, New Jersey, unpublished, 1980.
19. C. Gmelin and U. Rist. Active Control of Laminar-Turbulent Transition Using Instantaneous Vorticity Signals at the Wall. *Phys. Fluids*, pages 513–519, 2/2000.
20. J. Jeong and F. Hussain. On the identification of a vortex. *J. Fluid Mech.*, 285:69–94, 1995.